A Method for In-Process Failure Prediction in Cold Upset Forging

O. Ettouney

D. E. Hardt

Department of Mechanical Engineering,
Massachusetts Institute of Technology,
Cambridge, Mass. 02139

This paper addresses the prediction of plastic tensile instability and ductile fracture of a specimen undergoing a compression test (simple upsetting). The method used to predict failure is based primarily on Thomason's approach for predicting tensile plastic instability in compression tests. However, to apply this method to in-process prediction, a means for calculating the flow stress-strain properties from in-process measurements is needed. A method is introduced that is derived from Bridgman's correction factor for effective stress after necking occurs in the tensile test, but with a different approach that is suitable for compression specimens. The new correction factor enables one to correct the effective stress after barreling occurs, which eliminates the need for an ideal test (without barreling) to find the effective stress of a specimen. The results were in agreement with those derived from an ideal compression test. Stress data found using this correction factor was then used to predict failure using Thomason's method.

Introduction

Forging is basically a compression process and is classified by the geometry and by the type of equipment used. Forging may be done in open or closed dies; open die forgings are nominally struck between two flat surfaces while closed die forgings are formed in die cavities (Fig. 1 (*a*, *b*)). The simplest operation in forging is upsetting (Fig. 2). The process is generally limited to cylindrical workpieces whose length, because of the tendency to buckle, is usually less than three times their diameter. Barreling takes place (Fig. 2(*c*)) because of friction between the workpiece and the die that introduces radial shear stresses at the interface.

The quantitative study of simple compression in upsetting is central to the understanding of the behavior and characteristics of the process. Three basic questions arise with regard to this deformation process [1]: 1) What is the relationship among force required, material properties, and process variables; 2) how is the metal deformed throughout the workpiece; and, 3) how much can the height of the specimen be reduced before it begins to fail? The first question is significant because the change in the mechanical properties of an element in the workpiece depends on the degree of deformation. The relevance of the second question is self-evident in view of the type of data required for the design of forging equipment. The third question is representative of the important and complex area of formability in materials processing and has direct bearing on various factors, such as choice of workpiece material and selection of process variables to accomplish a given task.

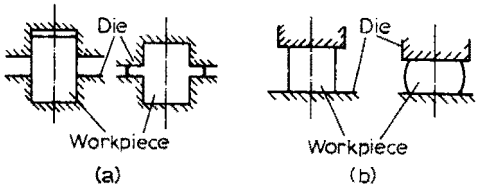

Fig. 1(a) Closed die forging process; (b) open die forging process

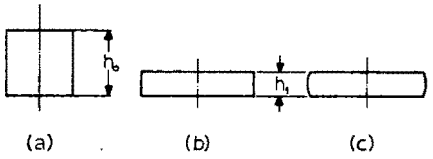

Fig. 2(a) Before; (b) after, without friction; (c) after, with friction

The objective of the present work is to *predict* failure of specimens undergoing compression so as to permit maximum deformation before unloading and stress relieving. The aim is to use data taken during the process (geometry configuration and applied load) to reach this prediction, so that on-line failure avoidance can be accomplished.

The basis of this prediction is the failure detection method of Thomason [9], which essentially states that failure will occur soon after the onset of tensile plastic instability at the surface of the material. To apply this method, the state of stress at the equatorial surface of the cylinder must be known. In this paper, a method for determining flow stress characteristics of a cylindrical compression specimen is introduced, so that the state of stress at the surface can be found. The novelty of this method is that flow stress is determined using measurements that can be made in-process, i.e., compression force, height reduction, and bulge radius.

Contributed by the Production Engineering Division for presentation at the Design and Production Engineering Technical Conference, Dearborn, Mich., September 11-14, 1983, of THE AMERICAN SOCIETY OF MECHANICAL ENGINEERS. Manuscript received at ASME Headquarters, December 27, 1982. Paper No. 83-Prod-6.

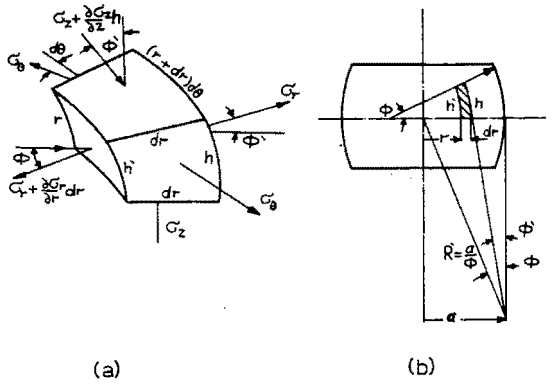

(a) (b)

Fig. 3 Approximate state of stress in the neighborhood of the maximum section of the bulge of a compression specimen; (*a*) stresses on element; (*b*) element in the bulge

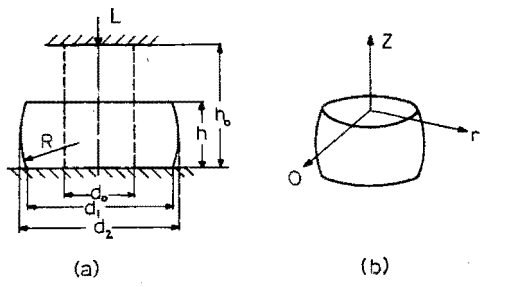

(a) (b)

Fig. 4(*a*) The "ordinary" compression test; (*b*) the three main directions (*a*, *θ*, and *r*)

Background

Stress-Strain Relations. In upset forging of cylinders, the stress distribution is uniform, and assuming a perfectly plastic material, the stress is equal to the uniaxial (compressive) yield strength of the workpiece material in the absence of friction (Fig. 2(*b*)) (ideal compression) or

$$\bar{\sigma} = \sigma_z = \frac{4L}{\pi d^2} \quad \sigma_r = \sigma_\theta = 0$$

Owing to the initial isotropy, the natural strains at a particular stage of the test are:

$$\epsilon_z = \ln\left(\frac{h}{h_0}\right), \quad \epsilon_r = \epsilon_\theta = -\frac{\epsilon_z}{2}$$

and the effective strain

$$\bar{\epsilon} = -\epsilon_z = \ln\left(\frac{h_0}{h}\right)$$

When friction develops one cannot use the previous "ideal" relations to find the effective stress-effective strain during a compression test. In the past, investigators have taken two approaches to solving this problem. In one, the friction during the process is determined from a separate test, then used to calculate the effective stress using analytical formulas [2-5], where the other approach derives the stress-strain relation from an ideal (frictionless) compression test and uses these results for a nonideal test (with friction) [6].

Schroeder and Webster [2] is a good example of the first group. They studied the effect of friction, area, and thickness on pressures required in the process of press-forging of thin sections. Their results, in which they introduced the nondimensional equations of pressure distribution on the interfacial surfaces under three different cases of friction, have been represented graphically. The solution for one value of the coefficient of friction depends on the values of the two other nondimensional ratios. Friction values were obtained from a separate test.

Bridgman [6] is at the head of the second group. He introduced a method for avoiding the effect of increasing nonuniformity of stress and strain caused by bulging as compression progresses. The method suggests performing the compression in stages, each followed by machining of the specimen back to the original proportions with continual decrease in the absolute size. A disadvantage of this method is that stress and strain do not increase monotonically, and disturbances are introduced by the stepwise release and reapplication of stress. However, and as Bridgman stated, these disturbances arise anyway from nonuniformity when a large compression is made in a single stage. This method was apparently first applied by Taylor and Quinney [7] to a study of copper.

Failure Prediction in Compression. A state of tensile plastic instability occurs when the rate of decrease in the cross-sectional area of an element and the rate of increase in the tensile component of stress reach a point where the load-carrying capacity of the element starts to decrease with continued deformation. When a cylindrical specimen is deformed in uniaxial compression the circumferential stress component on the equatorial free surface becomes increasingly tensile as "barreling" develops [8,9]. It is therefore possible for tensile instability to occur at some stage in the process of compression.

Many investigators have done work in this area and have developed different methods for predicting instability and fracture in compression tests. For example Kuhn [10] observed that unexpected deviations from smooth strains at the equator preceded surface failure. Shaw [11] introduced the maximum active tensile strain criterion which assumes that fracture will occur when the active tensile strain, ϵ'_θ, reaches a critical value, $\epsilon'_\theta{}^*$, where the active strain is defined as the actual strain minus the Poisson component of strain due to an orthogonally oriented principal stress, or

Nomenclature

$\bar{\sigma}$ = the effective stress $\equiv \frac{1}{2}[(\sigma_z-\sigma_r)^2 + (\sigma_r-\sigma_\theta)^2 + (\sigma_\theta-\sigma_z)^2]^{1/2}$, N/m^2(Psi)

$\sigma_z,\sigma_r,\sigma_\theta$ = axial, radial, and circumferential principal stress components, respectively, N/m^2 (Psi)

L = the applied load, N (lbf)

d = the current diameter in an ideal compression test without friction, m (in.)

$\epsilon_z,\epsilon_r,\epsilon_\theta$ = axial, radial, and circumferential principal strain, respectively

$\bar{\epsilon}$ = effective strain

h_0,h = initial and current height of cylindrical specimen, respectively, m (in.)

K = the current slope: $\equiv -d\epsilon_z/d\epsilon_\theta$

$d\epsilon_z,d\epsilon_r,d\epsilon_\theta$ = axial, radial, and circumferential principal strain increments, respectively

R = radius of the bulge, m (in.)

d_1,d_2 = minimum and maximum diameters of a bulged specimen, m (in.)

I = calculated point of tensile instability at equatorial free surface

F = observed point of macroscopic fracture at equatorial free surface

C' = bulge correction factor

$$\epsilon'_\theta \equiv 1.33(\epsilon_\theta + \epsilon_z/2)$$

and $\epsilon'_\theta > \epsilon'^*_\theta$ at fracture.

An approximate solution for the conditions for instability on the equatorial free surface of a compression specimen was introduced by Thomason [12]. He analyzed the equilibrium conditions of a thin ring element and deduced that instability will occur when

$$\frac{d\sigma_\theta}{d\epsilon_\theta} = \sigma_\theta(2-K), \quad \text{where } K \equiv \frac{-d\epsilon_z}{d\epsilon_\theta}$$

The method is easy to apply, and most of the required parameters are directly measurable from the test.

Approximate Solutions for Stresses Developed in Compression Test in the Presence of Barreling: Bulge Correction Factor

In order to apply Thomason's predictor, the surface stresses must be known. These can be found if the effective stress on the specimen at any time is known. Methods for finding this stress involve premeasurement of friction properties (as detailed above) and are thus impractical for on-line use. A method for finding the effective stress is introduced here that uses in-process measurements (force, height reduction, and bulge dimensions). This method is based on Bridgman's correction factor [6] used to determine the effective stress in the neck of a cylindrical tensile test specimen. A new correction factor is derived from the same arguments that have been used for necking in the tensile test, but in a way suitable for compression.

Referring to Fig. 3, it is assumed that a cylindrical specimen is being plastically deformed between two parallel-faced dies. As the thickness of the specimen is reduced, the major radius is increased. It is further assumed that the material is homogeneous and isotropic in its properties. Also, the principal stresses are assumed to be constant on the faces. Principal stresses are justified because the shearing stresses in the neighborhood of the maximum section must be negligible, since these stresses, because of symmetry, are zero at the maximum section of the bulge itself.

A detailed derivation of the compression test "correction factor" is presented in Appendix. The result is given by:

$$\bar{\sigma} = (\sigma_z)_{ave}\left\{\left[1 - \frac{2R}{d_2}\right]\ln\left[1 - \frac{d_2}{2R}\right]\right\}^{-1} \tag{1}$$

where

$$\sigma_{z_{ave}} = \frac{4L}{\pi d_2^2},$$

and the correction factor, C', which accounts for the presence of friction, is given by:

$$C' = \left\{\left[1 - \frac{2R}{d_2}\right]\ln\left[1 - \frac{d_2}{2R}\right]\right\}^{-1} \tag{2}$$

(This is of the same form as Bridgman's correction factor for stresses in the necked section of a uniaxial tensile specimen except for the sign of R.) The essential feature of equations (1) and (2) is that $\bar{\sigma}$ is easily computed given the compressive load (L), and the correction factor C', and the bulge radius R. Notice that if there is no friction, $R = \infty$ and $C' = 1.0$.

Experiments

A series of experiments were performed to: 1) test the validity of the compression bulge radius correction factor, and 2) use the effective stress data, calculated using equation (2), in Thomason's plastic instability criterion to predict failure.

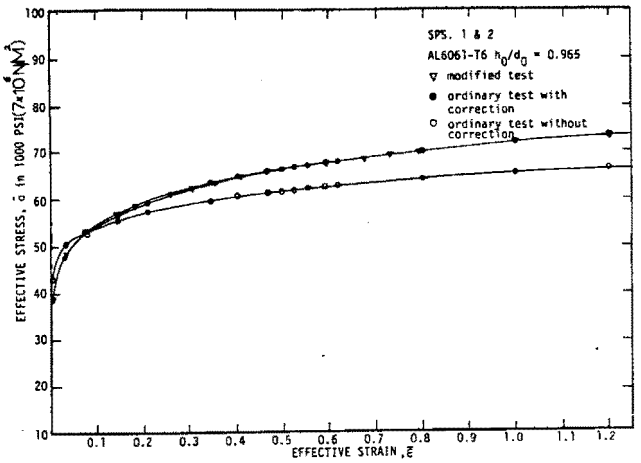

Fig. 5 Compression test results, specimens 1 and 2

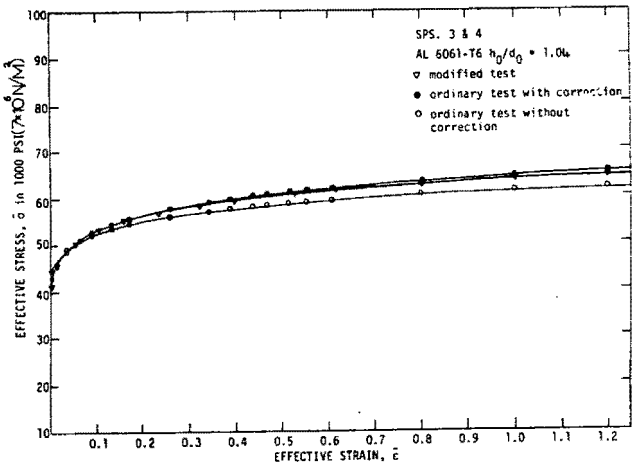

Fig. 6 Compression test results, specimens 3 and 4

Part 1: Effective Stress

Experimental Procedures and Measurements. Compression tests were carried out on a 530,000 N (60-t) universal testing machine. The specimens were upset between flat parallel dies mounted on a die subset placed on the testing machine. Two different friction conditions were utilized:

(*a*) polished dies with lubricant (oil-Moli #3) applied before each increment of deformation (for the zero friction – nonbarreling test), and

(*b*) polished dies without lubricant (for the ordinary test in the presence of friction and barreling).

The solid cylinders were prepared from commercially available aluminum of two alloys: Al 6061-T6 and Al 1100. Specimens were cut (from different bars) into different lengths giving height-to-diameter ratios of 0.965, 1.04, 1.15, 1.27, and 1.43, and they were used without any heat treatment in both tests (*a* and *b*).

The stress-strain measurements for the cylinders in compression were obtained according to the test to be performed (*a* or *b*). Axial and hoop strain measurements were made with a micrometer to an accuracy of 2.54×10^{-6} m (0.0001 in.). Three different methods were used for calculating the stresses: 1) In the zero friction – no-barreling test, the effective stress is simply the applied load over the area; 2) in the ordinary test (in the presence of barreling and friction), the effective stress is calculated by using the bulge correction factor (equation (2)); and 3) the average stress was calculated without the bulge correction factor based on the average diameter.

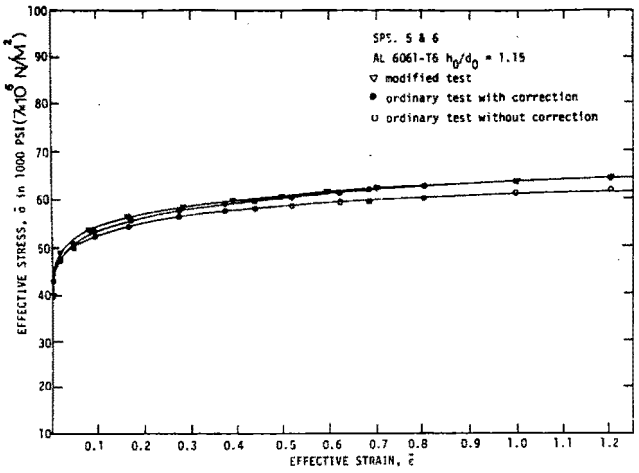

Fig. 7 Compression test results, specimens 5 and 6

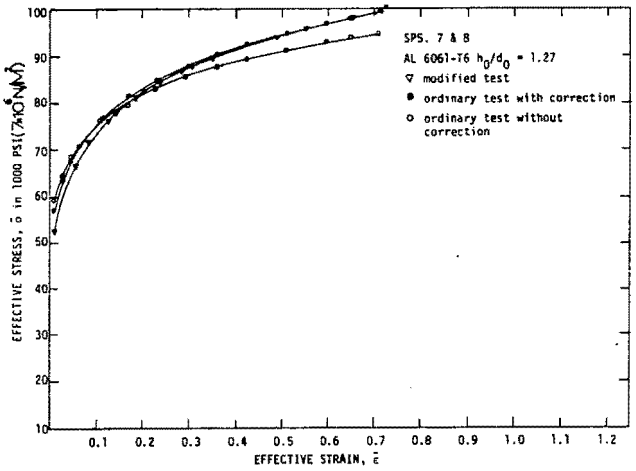

Fig. 8 Compression test results, specimens 7 and 8

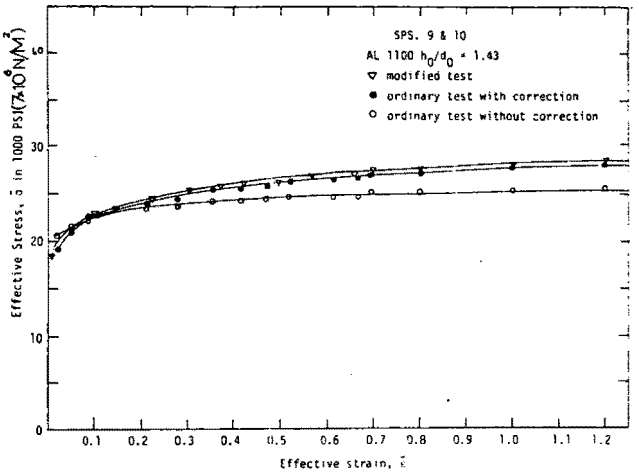

Fig. 9 Compression test results, specimens 9 and 10

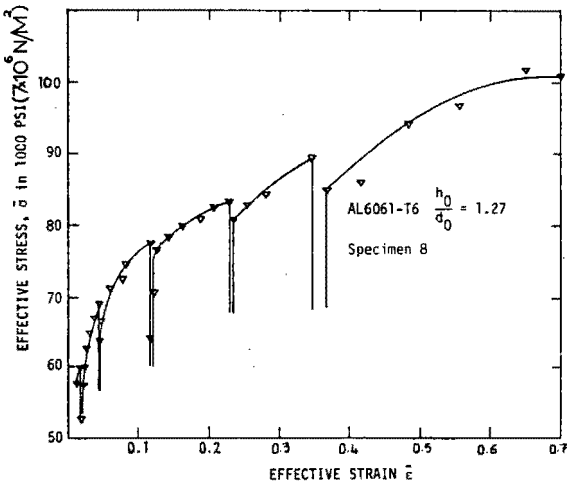

Fig. 10 Complete data from a modified test. Remachining occurred after each unloading cycle.

The bulge curvature R was calculated using two methods based on Kulkarni and Kalpakjian [13], which depends on using templates of known radii to measure the curvature, and an empirical formula [14], which relates the radius of curvature to the minor and major diameters (d_1 and d_2, respectively) and the height (Fig. 4):

$$R = \frac{h^2 + (d_2 - d_1)^2}{4(d_2 - d_1)}.$$

The second method is more practical, but the first method is also used as a check of the validity of the empirical formula.

Two different sets of experiments were performed, one based on running compression tests without the bulge correction factor discussed earlier, and the second based on Bridgman's modified test, which avoids nonuniformity by performing the compression in stages remachining the specimens back to the original proportions. (This latter procedure produced the "exact" data which the corrected data from tests with friction should mimic.)

Ten specimens were used, five for each experiment. Compression was done in stages, each differing by 4500 N (1000 lbf) from the other. Deformation was carried to a range between 45–70 percent for all the tests. In Figs. 5 to 9, the effective stress from the experiment and the average stress are shown as a function of the corresponding strains. The effective stress results from the ordinary test and by using the bulge correction factor behaves essentially the same as those from the zero friction – nonbarreling test. The deviation between the two is negligible in most cases, and the maximum difference is less than 7×10^6 N/m^2 (1000 Psi). The average stress, on the other hand, behaves in a different way. It decreases and deviates from the others after a strain of 0–1 and reaches a maximum difference of about 41×10^6 N/m^2 (6000 Psi). One more interesting thing about the curves of Figs. 5-9 is that the effective stress-effective strain behavior differs from one another for the same material. Usually at the same conditions (temperature, loads, and geometry) the effective stress-effective strain relationship is the same for the same material. In these experiments, different bars with different diameters were used, which is possibly the reason for this behavior.

Figure 10 gives all the data points for an ideal (zero bulging) test, showing that the effect of releasing load and reloading is a depression of the yield point below that reached in the previous application of stress. The interval between release and reapplication of load varied between half an hour and one day, with no apparent correlation between the interval of testing the excess or defect of yield point.

Conclusions. The experiments indicate that the effective stress results from the ordinary test by using the bulge correction factor to behave in a similar way to the zero friction – no-barreling test. The deviation is negligible between the two parts in most of the experiments.

Part II: Failure Prediction. To test the validity of the new

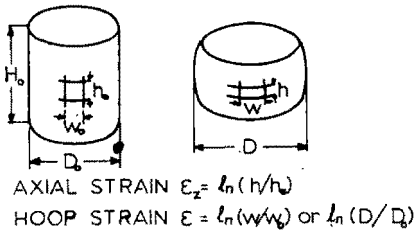

Fig. 11 Schematic of upset grids for strain measurements

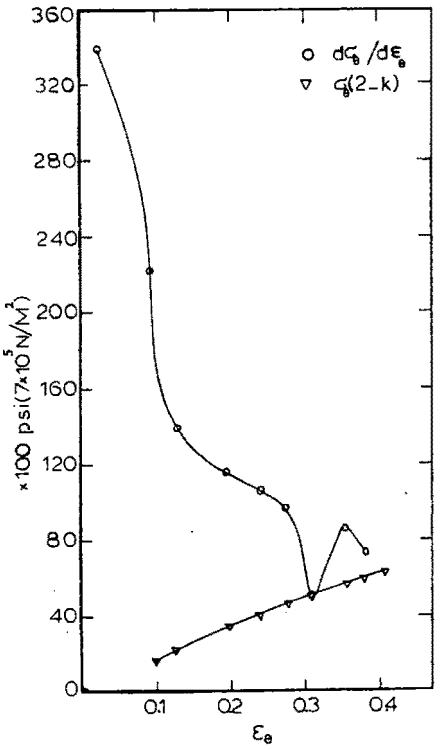

Fig. 12 Failure prediction parameters as a function of ϵ_θ

stress correction factor, failure prediction was used, along with surface strain increment measurements, in the following experiment to compute Thomason's plastic instability criterion. A number of compression tests, with various combinations of specimen geometry, were carried out to the point of fracture on the barreled surface, thus giving a wide variation in the history of the stress components and the strain increments at the equator.

The solid cylinders were prepared from commercially available 13×10^{-3}m- (1/2 in.)-dia aluminum (6061-T6). Specimens were cut into five different lengths, giving height-to-diameter ratios of 1.37, 1.29, 1.25, 1.19, and 0.94. The specimens were not given any heat treatment. (The effective stress is calculated by using the bulge correction factor after barreling occurs.) Compression tests were carried out on a 530,000 N (60 t) universal testing machine. The specimens were upset between flat parallel dies mounted on a die subset placed on the testing machine. The tests were carried out without lubrication.

For strain measurements, marks were indented at the midheight of the specimens, shown schematically in Fig. 11. Axial and hoop strain measurements were made with a toolmaker microscope to an accuracy of 2.54×10^{-6} m (0.0001 in.), with calculations in accordance with Fig. 12. The stress component at any stage of deformation on the free surface of the cylinder is calculated by the use of Levy-Mises equations, according to

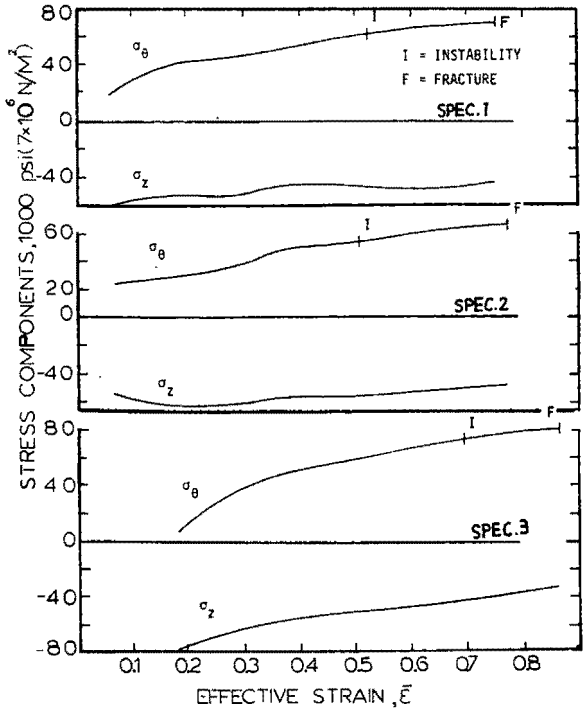

Fig. 13 Variation of equatorial free surface stress components during compression for specimens 1, 2, and 3 and without lubrication

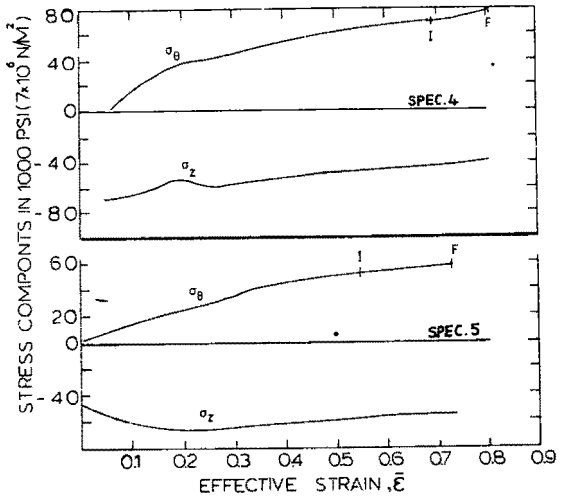

Fig. 14 Variation of equatorial free stress components during compression for specimens 4 and 5 and with friction

$$\sigma_\theta = \frac{\bar{\sigma}}{\sqrt{3}} \frac{2+K}{\sqrt{1+K+K^2}}$$

$$\sigma_z = \frac{\bar{\sigma}}{\sqrt{3}} \frac{1+2K}{\sqrt{1+K+K^2}}$$

The effective stress $\bar{\sigma}$ was calculated for every test using the correction factor developed above. The current slope, K, was calculated according to $K = -d\epsilon_z/d\epsilon_\theta$. The ϵ_z and the ϵ_θ principal strains, calculated from the equatorial grid measurements (Fig. 12), give scatter values which make any direct determination of the K value highly inaccurate. This problem was overcome by assuming a power function relationship between ϵ_z and ϵ_θ. The K values were obtained by differentiating this function for ϵ_z with respect to ϵ_θ.

Determination of point of instability was measured ac-

Table 1 Various quantities at fracture

Specimen	$\bar{\epsilon}$	ϵ_θ	$-\epsilon_z$	σ_θ Psi*	$-\sigma_z$ Psi*	$\bar{\sigma}$ Psi*
1	0.7477	0.4250	0.4926	70,193	44,820	100,408
2	0.7750	0.4005	0.4728	64,821	51,422	100,892
3	0.8614	0.4697	0.5863	80,997	34,125	102,418
4	0.8059	0.4395	0.5359	79,966	38,003	101,454
5	0.7319	0.4052	0.5390	60,573	54,939	100,076

*1 Psi = 7×10^3 N/m^2

Table 2 Tensile work to fracture and post-instability strain to fracture, no lubrication

H_0/D_0	effective strain to point of instability	effective strain from instability to fracture
1.379	0.4611	0.2265
1.298	0.4859	0.2657
1.259	0.5820	0.1665
1.191	0.6362	0.1136
0.948	0.5475	0.1802

cording to Thomason's method of predicting failure in compression [12]. The condition for tensile plastic stability under an internal pressure is

$$\frac{d\sigma_\theta}{d\epsilon_\theta} = \sigma_\theta(2-K) \tag{3}$$

According to equation (3), two conditions for instability can be recognized: 1) If $K<1$, instability will occur under an internal pressure, and 2) if $K>1$, instability will occur first under the action of σ_θ. In the present work, K was always less than one.

The method adopted here to determine the point of instability was to plot graphs of the circumferential stress σ_θ and the surface strain increment ratio $(2-K)$ against the circumferential strain ϵ_θ. By trial and error, a point along the σ_θ base-line could be found at which the tangent to the σ_θ curve had a gradient of σ_θ $(2-K)$, thus giving the theoretical point of tensile instability (see Fig. 12).

Experimental Results and Discussion

The stress components on the equatorial free surface were calculated from the strain measurements and are plotted against the compression strain $\bar{\epsilon}$ for the various conditions in Figs. 13 and 14. All various quantities at fracture of the experiments are given in Table 1. The results in Table 2 show that the effective strain varies considerably over the range 0.461 to 0.636 from the start of compression to the estimated point of tensile instability, for the various test conditions. However, the effective strain from instability to the point of fracture varies only slightly over the range 0.113 to 0.265. These results suggest that during stable plastic flow there is very little contribution to the conditions which cause ductile fracture; but when tensile instability occurs, ductile fracture progresses rapidly [12].

The estimated point of instability for each compression test was determined by means of equation (3) and is indicated by point 1 in Figs. 13 and 14. The effect of experimental errors on the calculated values of ϵ_z and ϵ_θ were estimated to be less than ± 7 percent. The resultant error in the σ_θ stress components was therefore less than ± 1 percent.

Fracture occurred at 45 deg for all the specimens which means that the axial stress on the equatorial surface was compression at this point [12].

Summary

As a result of the present study, the following results can be stated.

1 The effective stress can be found during normal compression tests with friction by using a bulge correction factor that can be applied using in-process measurement. This step eliminates the separate test that is usually performed to find the effective stress.

2 The new correction factor is based mainly on arguments similar to those Bridgman used to find a correction factor for stresses in the neck of a tensile specimen.

3 The effective stresses found by use of the new factor behaved in a similar manner to those found by Bridgman's modified compression test (ideal compression without barreling) (Figs. 5 to 9).

4 Thomason's method of predicting tensile instability and ductile fracture was applied to normal tests using the stress prediction method and the results were in agreement with Thomason's results. The main difference between the present work's approach and Thomason's is that the effective stress was found from in-process measurements and was used directly in the method without the need for a separate test.

References

1 Kalpakjian, S., *Mechanical Processing of Materials*, D. Van Nostrin Company, Inc., Princeton, N. J.

2 Schroeder, W., and Wevster, D. A., "Press-Forging of Thin Sections: Effect of Friction, Area and Thickness of Pressure Required," ASME *Journal of Applied Mechanics*, Vol. 16, 1949, p. 289.

3 Kôbayashi, S., Herzog, R., Lapsley, J. T., Jr., and Thomsen, E. G., "Theory and Experiments of Press Forging Axisymmetric Parts of Aluminum and Load," *Trans. ASME*, Vol. 81, 1958, p. 228.

4 Kobayashi, S., MacDonald, A. G., and Thomsen, E. G., "Some Aspects of Press Forging," *Int. J. Mech Sci.*, 1960, pp. 232-230.

5 MacDonald, A. G., Kobayashi, S., Thomsen, E. G., "Some Problems of Press Forging Lead and Aluminum," ASME JOURNAL OF ENGINEERING FOR INDUSTRY, Vol. 82, 1960, pp. 246-252.

6 Bridgman, P. W., *Studies in Large Plastic Flow and Fracture*, McGraw-Hill, 1952, pp. 9-37, 38-86, 181.

7 Taylor, G. I., and Quinney, H., *Proc. Roy. Soc.*, London, Vol. 143, 1933-1934, pp. 307-326.

8 Kudo, H., and Aoi, K., "Effect of Compression Test Conditions upon Fracturing of a Medium Carbon Steel-Study on Cold-Forgeability Test: Part II," *J. of Japan Soc. of Tech. in Plasticity*, Vol. 8, 1967, pp. 17-27.

9 Thomason, P. F., "The Use of Aluminum as an Analogue for the History of Plastic Flow, in Studies of Ductile Fracture Criteria in Steel Comparison Specimens," *Int. J. Mech. Sci.*, Vol. 10, 1968, p. 501.

10 Kuhn, H. A., and Lee, P. W., "Strain Instability and Fracture at the Surface of Upset Cylinders," *Met. Trans.*, Vol. 2, 1971, pp. 2197-3242.

11 Shaw, M. C., "Forming Limit Diagrams for the Cold Forging of Metals," *Proceedings, Seventh NAMRC*, May 1979.

12 Thomason, P. F., "Tensile Plastic Instability and Ductile Fracture Criteria in Uniaxial Compression Tests," Department of Mechanical Engineering, University of Salford, 1968.

13 Kulkarni, K. M., and Kalpakjian, S., "A Study of Barreling as an Example of Free Deformation in Plastic Working," ASME Paper No. WA-68/Prod-6, 1968.

14 Horton, H. L., Ryffel, H. H., and Schubert, P. B., *Machinist's Handbook*, 16th edition, The Industrial Press, N.Y., 1959, p. 152.

APPENDIX

Approximate Solutions for Stresses Developed in a Compression Test in the Presence of Barreling

The following equation results from the condition of equilibrium in the r-direction in Fig. 3:

$$\left(\sigma_z + \frac{\partial \sigma_z}{\partial z} h\right) \sin\phi' \left(r + \frac{dr}{2}\right) d\theta dr$$

$$- \left(\sigma_r + \frac{\partial \sigma_r}{\partial r} dr\right)(dr + r) d\theta h - (\sigma_\theta \sin d\theta) + \sigma_r h r d\theta = 0 \tag{1}$$

Geometrical equations for h and h' can be derived from Fig. 3 in terms of R, $R' = a/\phi$, ϕ and ϕ':

$$h = R\phi - \frac{a}{\phi}(\cos\phi' - \cos\phi)$$

$$h' = R\phi - \frac{a}{\phi}[\cos(\phi' + d\phi') - \cos\phi) \tag{2}$$

Introduction of equation (2) into equation (1) and neglecting all terms except those of lowest order yields:

$$\sigma_z \frac{r^2}{a} = \sigma_r \left(\frac{3}{2}\frac{r^2}{a} - \frac{a}{2} + R\right) - r\frac{d\sigma_r}{dr}\left[\frac{1}{2}\left(\frac{a^2 - r^2}{a}\right) - R\right]$$

$$+ \sigma_\theta \left[\frac{1}{2}\left(\frac{a^2 - r^2}{a}\right) - R\right] \tag{3}$$

Symmetrical deformation requires that on the maximum section

$$d\epsilon_\theta = d\epsilon = -\frac{1}{2} d\epsilon_z \tag{4}$$

From the plasticity equations it follows that

$$\sigma_r = \sigma_\theta \tag{5}$$

Introduction of equation (5) into the effective stress equations yields

$$\bar{\sigma} = \sigma_z - \sigma_r \tag{6}$$

Assuming that $\bar{\sigma}$ = constant on the bulge and introducing this into equation (3):

$$\frac{d\sigma_r}{dr}\left[\frac{1}{2}\left(\frac{a^2 - r^2}{a^2}\right) - R\right] + \frac{r\bar{\sigma}}{a} = 0 \tag{7}$$

Separation of variables and introduction of the boundary condition $r = a$ at the free surface

$$\sigma_r = 0 \quad \bar{\sigma} = \sigma_z \tag{8}$$

permit ready integration, and the stresses become:

$$\sigma_r = \bar{\sigma} \ln\left(\frac{a^2 - 2ar - r^2}{-2ar}\right) \tag{9}$$

$$\sigma_z = \bar{\sigma}\left[1 + \ln\left(\frac{a^2 - 2aR - r^2}{-2aR}\right)\right] \tag{10}$$

Introduction of σ_z into the condition that the load across any section of the bar is given by

$$F = 2\pi \int_0^a \sigma_z r dr = \pi a^2 (\sigma_z)_{\text{ave}} \tag{11}$$

resulting in:

$$\pi a^2 (\sigma_z)_{\text{ave}} = \pi \bar{\sigma}(a^2 - 2aR) \ln\left(1 - \frac{a}{2R}\right) \tag{12}$$

from which the relation between the average axial stress $(\sigma_z)_{\text{ave}}$ and $\bar{\sigma}$ is given by

$$\bar{\sigma} = (\sigma_z)_{\text{ave}} \left[\left(1 - \frac{2R}{a}\right) \ln\left(1 - \frac{a}{2R}\right)\right]^{-1} \tag{13}$$

Thus the correction factor for converting the average stress into a correct effective stress is given by the factor:

$$C' = \left[\left(1 - \frac{2R}{a}\right) \ln\left(1 - \frac{a}{2R}\right)\right]^{-1}$$